Two-Dimensional Visible/Near-Infrared Correlation Spectroscopy Study of Thermal Treatment of Chicken Meats

Yongliang Liu,[†] Yud-Ren Chen,*[,†] and Yukihiro Ozaki[‡]

Beltsville Agricultural Research Center, Agricultural Research Service, U.S. Department of Agriculture, Beltsville, Maryland 20705-2350, and Department of Chemistry, School of Science, Kwansei-Gakuin University, Uegahara, Nishinomiya 662-8501, Japan

The thermal treatment of chicken meats was investigated by generalized 2D visible/NIR correlation spectroscopy. Synchronous 2D visible correlation analysis revealed that there are at least two bands around 445 and 560 nm, decreasing in intensity with cooking time. The corresponding asynchronous spectrum indicated that the spectral intensity reduction of the two bands occurs before the intensity variation of the 475, 520, and 585 nm bands. It suggested that the 445 and 560 nm bands be assigned to deoxymyoglobin and oxymyoglobin, respectively, and at least one of the 475, 520, and 585 nm bands assigned to the denatured species (metmyoglobin) of myoglobin. Also, the asynchronous 2D NIR correlation spectrum indicated that C−H fractions are easily oxidized. In addition, strong correlation peaks correlating the bands in the visible, SW-NIR, and NIR spectral regions were observed and discussed.

Keywords: *Two-dimensional correlation analysis; visible/NIR spectroscopy; chicken meat; thermal treatment; myoglobin*

INTRODUCTION

Generalized two-dimensional (2D) correlation spectroscopy (Noda, 1993), which is an extension of the original 2D correlation spectroscopy proposed by Noda in 1986 (Noda, 1986, 1989, 1990), has recently received keen interest because it enables one to analyze the spectral intensity fluctuation as a function of many physical variables, for example, time and temperature (Ebihara et al., 1993; Nakano et al., 1993; Nabet and Pezolet, 1997; Ozaki et al., 1997; Sefara et al., 1997). Generalized 2D correlation spectra accentuate spectral features not readily observable in conventional one-dimensional spectra. It is possible to probe the specific order of the spectral changes taking place with the change of the controlling variables.

2D correlation spectroscopy has been applied widely as a universal spectral analytical method. For example, Ozaki and co-workers systematically investigated the temperature-dependent spectral variations of self-associated molecules, by using 2D IR, 2D near-IR (NIR), 2D Raman, and IR-Raman spectroscopic techniques, to probe the specific order of the spectral changes and establish band assignments (Noda et al., 1995, 1996a,b; Liu et al., 1996; Ozaki et al., 1997).

Visible/NIR spectroscopy has already found considerable applications in food and meat products (Williams and Norris, 1990; Burns and Ciurczak, 1992; Osborne et al., 1993). Common applications with meat include the quantitative prediction of not only chemical composition, such as fat and protein, but also physical characteristics, such as hardness and tenderness (Lanza, 1983; Mitsumoto et al., 1991; Ellekjaer et al., 1994; Park et al., 1998). In addition, it has also been developed to classify wholesome and unwholesome chicken carcasses (Chen et al., 1998) and to evaluate thermally induced changes in poultry meat products (Swatland, 1983; Chen and Marks, 1998). Chen et al. (1996a,b, 1998) applied it to the on-line classification of poultry carcasses at slaughter plants with an average of >94% in discriminating wholesome and unwholesome classes. Swatland (1983) reported that the reflectance spectra of raw and cooked chicken muscles in the 400−700 nm region exhibited large spectral changes around 560 nm due to the cooking effect, whereas Chen and Marks (1997, 1998) estimated the integrated time−temperature history of heat-treated chicken patties and further predicted their physical properties. Although these studies indicate that visible/NIR spectroscopy is feasible and promising in the quality control of raw and thermally processed poultry products, few studies have specifically related visible/NIR spectra to the chemical composition and structure of chicken meats.

It is well-known that heating during cooking results in extensive changes in the appearance and physical properties of chicken muscles (Swatland, 1983; Kinsman et al., 1994; Chen and Marks, 1997, 1998). These changes include the toughening and discoloration (from purplish red to grayish white) of the muscles, with toughening due to the denaturation of proteins and discoloration due to the oxidization of pigment heme group in myoglobin of muscle (Kinsman et al., 1994).

In this study, we have applied generalized 2D visible/NIR correlation spectroscopy to the cooking of chicken meats to correlate the absorption bands in different ranges. Visible/NIR spectra in the 400−2500 nm region of the chicken meats cooked over periods of 3−18 min at a constant convection temperature of 150 °C were measured. It is expected that the 2D approach may

* Author to whom correspondence should be addressed [Telephone (301) 504-8450; fax (301) 504-9466; e-mail cheny@ba.ars.usda.gov].

[†] U.S. Department of Agriculture.

[‡] Kwansei-Gakuin University.

10.1021/jf990662b CCC: $19.00
Published on Web 02/12/2000

elucidate cooking time-dependent spectral changes of cooked muscles both in the visible region of various states of myoglobin and in the NIR regions of the first, second, and third overtones of C−H, O−H, and N−H stretching modes in chicken compositions. Therefore, it may provide new insight into the heating-induced structural and composition changes of meat products in wider spectral ranges.

BACKGROUND

The mathematical background for the generalized 2D correlation spectroscopy has been described in detail by Noda (1993), and applications of the generalized 2D correlation approach to IR, NIR, and Raman spectral data have been widely reported (Ebihara et al., 1993; Nakano et al., 1993; Noda, 1996a,b; Nabet and Pezolet, 1997; Ozaki et al., 1997; Sefara et al., 1997).

The generalized 2D correlation spectra consist of synchronous and asynchronous correlation spectra. A synchronous 2D correlation spectrum characterizes the similarity between the sequential variations of spectral intensities. Autopeaks located at the diagonal position represent the extent of dynamic variations of spectral intensity at different wavelengths. Synchronous cross-peaks appear at off-diagonal positions. These occur if the basic trends of dynamic variations, observed at two different wavelengths of the cross-peak spectral coordinate, are similar. A positive cross-peak indicates that intensities at both wavelengths are either increasing or decreasing together, and a negative peak suggests that one intensity is increasing while the other is decreasing.

An asynchronous 2D correlation spectrum, which consists exclusively of off-diagonal cross-peaks, characterizes the difference between the time-dependent sequential variations of spectral intensities. Asynchronous cross-peaks appear if the basic trends of dynamic variations, observed at two different wavelengths of the cross-peak spectral coordinate, are dissimilar. From the positive or negative sign of an asynchronous cross-peak, it is possible to assign the specific sequence of events occurring at different times. A negative cross-peak indicates that the event (increase or decrease of intensity) observed at wavelength λ_1 occurs later than the event observed at wavelength λ_2. A positive asynchronous cross-peak indicates the opposite.

Throughout this paper, solid and dashed lines denote positive and negative cross-peaks, respectively, in synchronous and asynchronous spectra.

MATERIALS AND METHODS

Meat Sample and Thermal Treatment. The wholesome chicken carcass was obtained from a slaughter plant in Cordova, MD, and its condition was identified on-line by the Food Safety and Inspection Service (FSIS) inspectors. Fresh slices (1 cm thick and 3.8 cm diameter) were acquired from the bulk breast muscle of the chicken to fit into the spectrophotometer's quartz window-clad cylindrical cup. Prior to cooking, each slice was sealed in a polyethylene bag and kept at 0 °C.

The samples were cooked in a small convection oven (Equipex Sodir Model FC-26/34, Providence, RI) at a constant air temperature of 150 °C for 3, 6, 9, 12, 15, and 18 min. Once the cooking sample reached the target time, it was removed from the oven, and immediately its surface temperature was measured using a J-type thermocouple (Omega model HH21 microprocessor thermometer, Stamford, CT). It was then resealed in a polyethylene bag. As a result, the end-point temperatures after 3, 6, 9, 12, 15, and 18 min of cooking were 29.2, 44.6, 52.1, 63.1, 66.3, and 75.8 °C, respectively. After cooling to room temperature, visible/NIR spectra were collected.

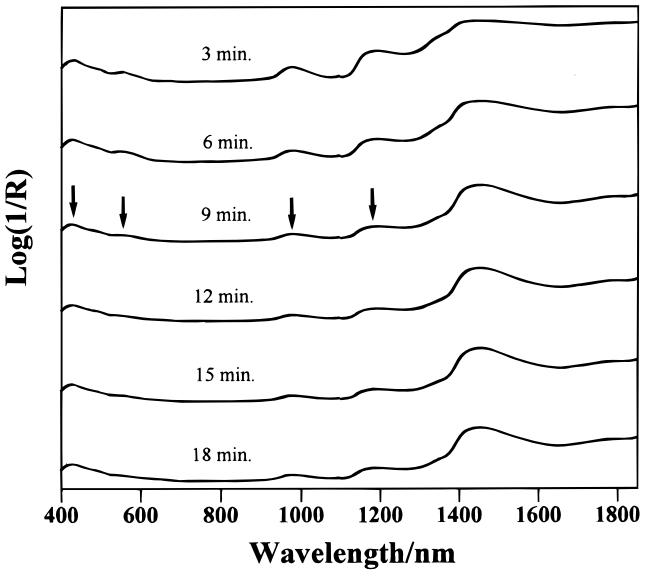

Figure 1. Time-dependent visible−NIR spectra in the 400−1850 nm region of chicken breast muscles from 3 to 18 min under an air temperature of 150 °C.

Spectroscopic Measurement and 2D Correlation Analysis. Visible/NIR reflectance spectra were collected using a scanning monochromator NIRSystems 6500 spectrophotometer (NIR Systems, Silver Spring, MD) equipped with a rotating sample cup. Before a spectrum of a piece of chicken meat was measured, a background spectrum was collected. Each spectrum, an average of 32 scans, was recorded over the 400−2500 nm wavelength range at 2 nm intervals.

The obtained spectra were transformed into .spc files. They were simply offset to zero using Grams/32 software (Galactic Industrious Corp., Salem, NH), and 2D correlations were performed using the KG2D correlation program (School of Science, Kwansei-Gakuin University, Nishinomiya, Japan) installed in Grams/32 software (Wang et al., 1998). In the 2D approach, dynamic (or difference) spectra, obtained by subtracting the average spectrum from each of the original spectra, were used to develop two correlation spectra commonly known as synchronous and asynchronous 2D correlation spectra.

The selection of the minimum threshold intensity level of the contour map is somewhat arbitrary. Thus, some of the fine features of the correlation spectrum could be omitted if the threshold is too high, whereas minor features arising from noise and baseline distortions may be overaccentuated if the selected threshold is too low. The minimum threshold of each contour line map was set to 30% of the maximum point of the map, unless otherwise stated.

RESULTS AND DISCUSSION

Visible/NIR Spectra of Cooked Chicken Breast muscles. Figure 1 shows the representative visible/NIR spectra in the 400−1850 nm region of the chicken breast muscles cooked for 3, 6, 9, 12, 15, and 18 min. Even with limited chemical composition and structural information of this chicken meat, preliminary band assignments in the 400−1850 nm region could be made by referring to other visible/NIR studies of meat, protein, fat, and water (Swatland, 1983; Lawrie, 1985; Price and Schweigert, 1987; Williams and Norris, 1990; Burns and Ciurczak, 1992; Osborne et al., 1993). Two bands appear at 445

and 560 nm in the visible region, and they are related to the presence of various states of myoglobin. Some hemoglobin in residual blood may also be present in a sample, but generally it is minimal and has little effect on the spectral characterization of wholesome muscle because the chicken carcass was well bled (Francis and Clydesdale, 1975). Although the band at 980 nm is commonly thought to be the second overtones of O−H stretching modes of water and alcohol molecules, it may also include contributions from the third overtones of C−H stretching modes of heme group in myoglobin as evidenced from the following discussion. Features between 1100 and 1300 nm are from the second overtones of the C−H stretching modes, whereas their first overtones appear in the 1600−1850 nm region. Bands in the 1300−1400 nm region are ascribed to combination bands of the C−H vibrations. Broad bands in the 1400−1600 nm region are due to the overlaps of the first overtones of the O−H/N−H stretching modes of self-associated and water-bonded OH/NH groups in meat compositions.

In Figure 1, it is noted that the intensities of the bands at 445, 560, 980, and 1195 nm decrease obviously with cooking time. This observation is consistent with other studies (Swatland, 1983; Chen and Marks, 1997, 1998). However, it is difficult to extract useful information from such broad and overlapped band features. Because absorption bands from the same chemical species may have very different absorptivities in three different wavelength ranges: (i) visible region, 400−700 nm; (ii) short-wave NIR (SW-NIR) region, 700−1100 nm; and (iii) NIR region, 1100−1850 nm (Silverstein et al., 1991; Bonanno et al., 1992), the application of 2D correlation analysis technique was attempted for the absorbance bands in these ranges.

2D Correlation Spectra of the Bands in the Visible, SW-NIR, and NIR Ranges. Parts A and B of Figure 2 show a contour line map and a three-dimensional (3D) representation, respectively, of the synchronous 2D correlation spectra of cooked chicken meats in the visible region. This optical region is one of the most interesting regions due to the presence of deoxymyoglobin and oxymyoglobin, which play important roles in the chemical, physical, and quality characteristics of meats (Lawrie, 1985; Price and Schweigert, 1987; Kinsman et al., 1994). By focusing on the correlation analysis within this narrow range, it is hoped that more distinctive spectral changes may emerge. Major autopeaks at the diagonal position are observed around 445 and 560 nm, and cross-peaks associated with the autopeaks are also observed at off-diagonal positions (Figure 2A). The appearance of the autopeaks means that the intensities of these two bands changed very significantly with cooking. Furthermore, the positive cross-peaks indicate that the cooking time-induced change in the spectral intensity of the band at 445 nm is similar to that of the 560 nm band. Also, Figure 2B reveals that the strong autopeak at 445 nm probably comes from deoxymyoglobin absorption due to its significant spectral intensity reduction.

Figure 2C depicts the asynchronous 2D correlation spectrum of cooked meat samples in the same spectral region. Major cross-peak pairs appear around 415, 425, 445, 475, 520, 560, and 585 nm. The positive asynchronous correlation peaks indicate that the cooking time-induced change of visible absorption intensities at 445 and 560 nm occurs before those at wavelengths of 415,

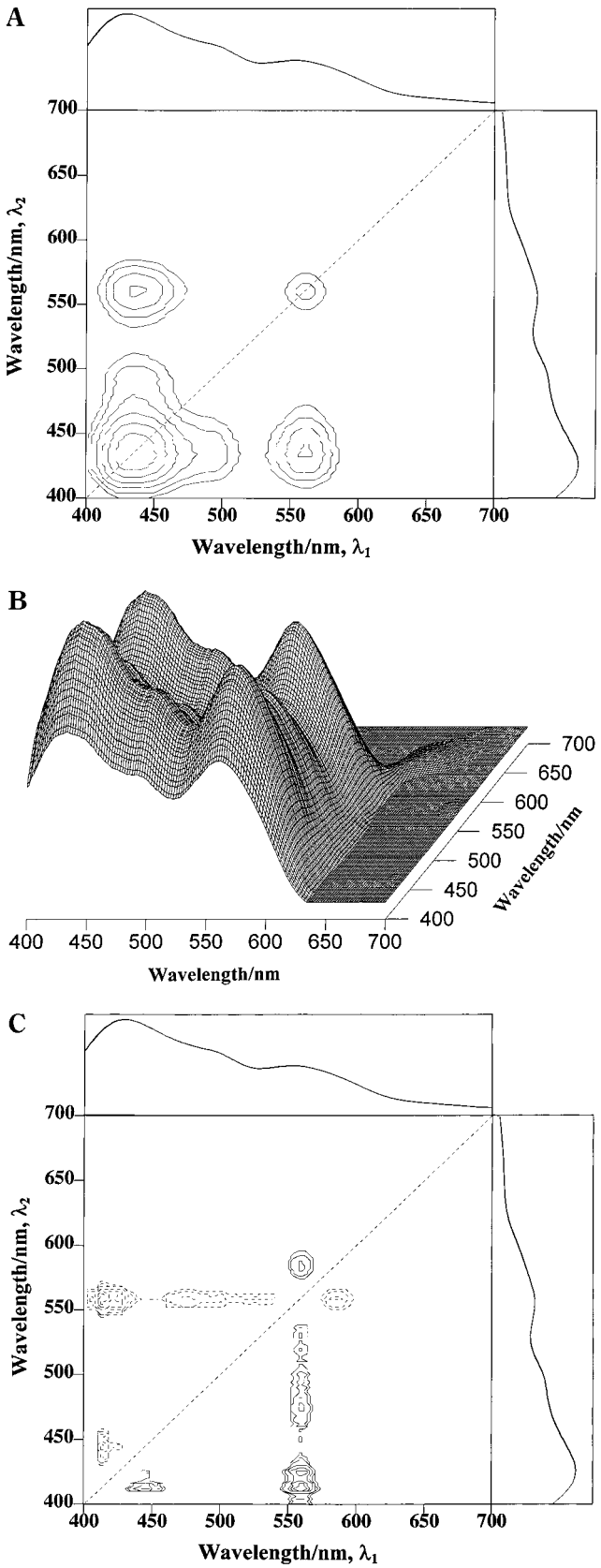

Figure 2. 2D correlation spectra of cooked chicken muscles in the 400−700 nm region: (A) synchronous contour line version; (B) synchronous three-dimensional (3D) version; (C) asynchronous contour line version. The average spectrum for the data set is plotted at the top and right of each plot.

425, 475, 520, and 585 nm. This strongly suggests that the 445 and 560 nm bands easily change their intensities due to heating effect and thus are probably related

to the color of meat, that is, the deoxymyoglobin and/or oxymyoglobin component (Lawrie, 1985; Price and Schweigert, 1987; Kinsman et al., 1994). It is interesting to note that the two spectral bands with the intensity changes occurring first as shown in the asynchronous 2D plot are the same two bands as shown in the synchronous cross-peaks. The development of cross-peaks in asynchronous 2D correlation implies the possible existence of the oxidized/denatured derivatives resulting from cooking. These asynchronous peaks characterize the intrinsic dissimilarity of temperature-dependent behavior of different absorption bands in the visible region.

In a separate study of wholesome and unwholesome chicken muscles (Liu et al., 2000), 2D correlation spectra revealed two significant autopeaks at 445 and 560 nm for wholesome and cadaver (improperly bled) carcasses and at 485 and 560 nm for diseased ones. Hence, it can be concluded that the bands at 445 and 560 nm are attributed to deoxymyoglobin and oxymyoglobin, respectively, and one or more bands at around 475, 520, and 585 nm may be possibly due to metmyoglobin. The other bands at 415 and 425 nm can be assigned to the Soret absorbance bands for oxymyoglobin and metmyoglobin (Swatland, 1989).

Figure 3 shows the synchronous and asynchronous 2D correlation spectra in the SW-NIR region. In this region, the bands are exclusively due to the second and/or third overtones of C−H, O−H, and N−H stretching vibrations and the combinations of C−H modes. Figure 3A shows that only an autopeak at 980 nm appears in the synchronous 2D SW-NIR spectrum. Along with the signs of asynchronous cross-peaks shown in Figure 3B, it indicates that the cooking time-induced change of absorption intensity at 980 nm occurs before the two bands near 910 and 1070 nm. It implies that the 980 nm band may arise from the pigment heme groups in deoxymyoglobin and oxymyoglobin, whereas 910 and 1070 nm bands are ascribed to the third overtones of C−H stretching modes and the C−H combination bands of components other than deoxymyoglobin and oxymyoglobin, respectively.

The synchronous 2D NIR spectrum shown in Figure 4A is constructed from the spectral region between 1100 and 1850 nm. In this spectral region, the bands generally are attributed to the first and second overtones of C−H stretching modes, the first overtones of O−H and N−H stretching modes, and the combinations of C−H vibrations. Figure 4A reveals that there are two dominating autopeaks around 1360 and 1655 nm. Positive cross-peaks are found at off-diagonal spectral coordinates between the 1655 nm band and the two NIR bands at 1195 and 1360 nm in this spectral region. This means that the thermally induced reduction in spectral intensity at 1655 nm is reasonably similar to those of the bands at 1195 and 1360 nm. In fact, they represent different band origins for the same species; that is, the bands at 1655 and 1195 nm are assigned to the first and second overtones of the C−H stretching modes, whereas the band at 1360 nm is assigned to the combinations of the same C−H vibrations.

Figure 4B depicts the asynchronous 2D NIR correlation spectrum in the same spectral region. The cross-peaks are located at the spectral coordinate near 1455 nm. Although this band is mainly due to the first overtone of O−H stretching vibrations of water, there are also contributions from the first overtones of N−H and O−H stretching modes of various meat constitutes, such as myoglobin and proteins. The result suggests that the cooking time dependence of the water band at 1455 nm is quite different from those of bands at 1195, 1360, and 1655 nm, which are due to C−H vibration modes. The signs of the cross-peaks indicate that as the cooking continued, the NIR band intensities at 1195, 1360, and 1655 nm changed before that of the OH band at 1455 nm did. Thus, the C−H fractions in meat denature and oxidize apparently more readily than water evaporates or hydrogen-bonded OH species dissociate. Because of the fast discoloration process upon cooking, it may be concluded that the C−H fractions are related to the pigment heme groups in deoxymyoglobin and oxymyoglobin. Therefore, both 1655 and 1195 nm bands can be attributed to the first and second overtones of the C−H stretching vibrations and the 1360 nm band to the combination modes of heme groups in deoxymyoglobin and oxymyoglobin.

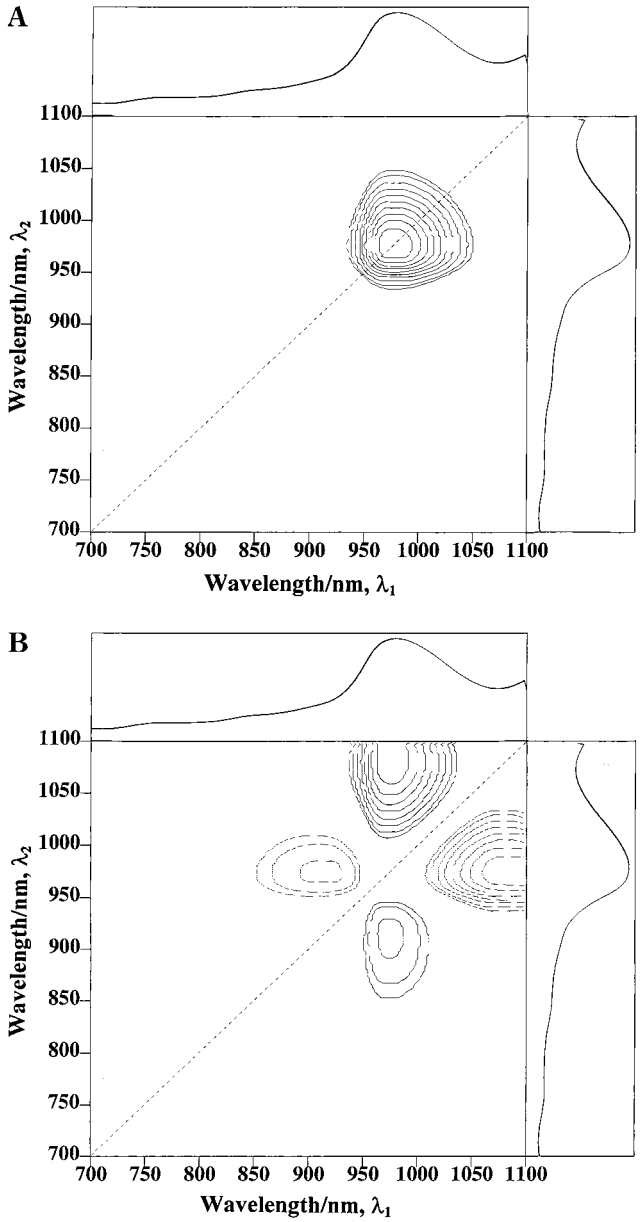

Figure 3. 2D correlation spectra of cooked chicken muscles in the 700−1100 nm region: (A) synchronous contour line version; (B) asynchronous contour line version. The average spectrum for the data set is plotted at the top and right of each plot.

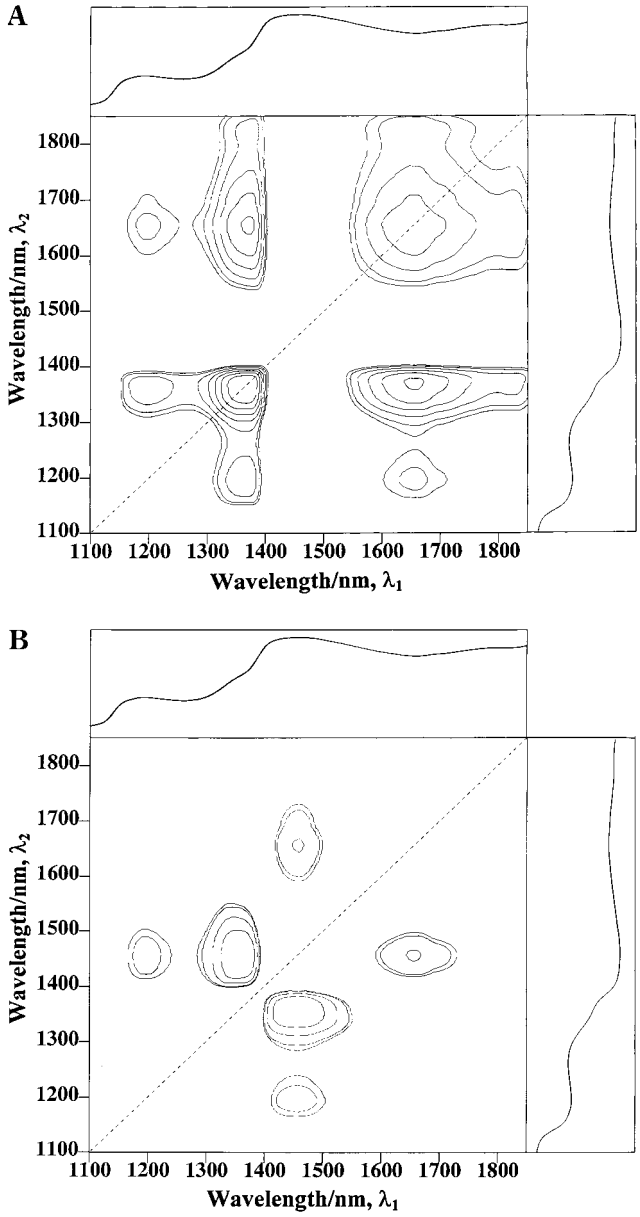

Figure 4. 2D correlation spectrum of cooked chicken muscles in the 1100−1850 nm region: (A) synchronous contour line version; (B) asynchronous contour line version. The average spectrum for the data set is plotted at the top and right of each plot.

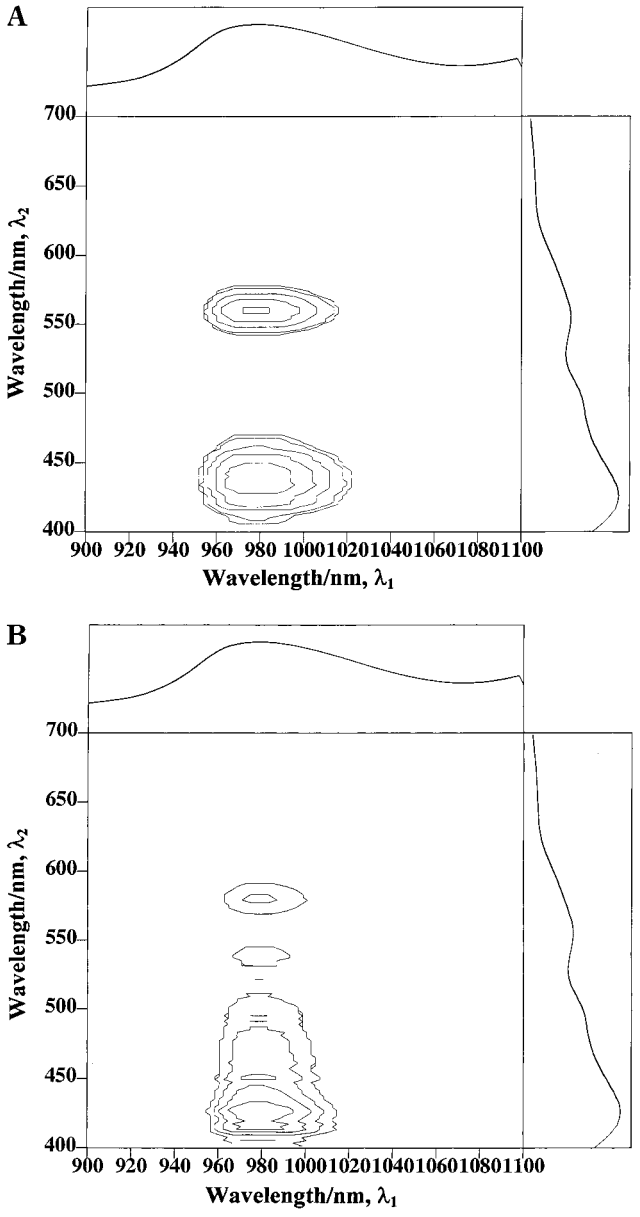

Figure 5. 2D correlation spectra of cooked chicken muscles in the off-diagonal region bounded by 400−700 nm (vertical) and 900−1100 nm (horizontal): (A) synchronous contour line version; (B) asynchronous contour line version. The corresponding portions of the average spectrum for the data set are plotted at the top and right of each plot.

2D Correlation Spectra of Correlating Bands in Different Spectral Ranges. *(a) Visible Region versus SW-NIR and NIR Regions.* Parts A and B of Figure 5, respectively, show the synchronous and asynchronous 2D correlations between the visible and SW-NIR regions. Figure 5A indicates that the change in the spectral intensity of the 980 nm band is synchronously correlated with those of visible bands located at 445 and 560 nm. The asynchronous spectrum in Figure 5B reveals additional absorption bands at 415, 425, 450, 540, and 575 nm, with intensity changes that occur later than those at 445 and 560 nm. Also, Figure 5B suggests that there is little asynchronicity between the 980 nm SW-NIR band and the 445 and 560 nm visible bands, indicating that the 980 nm band may be due to similar constituents from which the 445 and 560 nm bands originated.

The comparison of the absorption bands between the visible and NIR ranges is given in Figure 6. The changes in visible intensities of the bands at 445 and 560 nm (Figure 6A) coincide with those of NIR bands at 1195, 1365, and 1655 nm. The asynchronous spectrum in Figure 6B again indicates that the spectral fluctuation of the bands at 1195 and 1365 nm varies more quickly than those at 415, 425, 450, 540, and 580 nm, and the spectral intensity change of the 1455 nm band occurs later than those at 445 and 560 nm bands.

(b) SW-NIR Region versus NIR Region. The first, second, and third overtones of the C−H stretching vibrations in SW-NIR and NIR regions are compared in Figure 7. The strong and positive synchronous cross-peaks exist between the NIR band intensity changes around 1195, 1360, and 1655 nm and the one at 980 nm (Figure 7A). The cooking time-dependent behaviors of the band at 980 nm and those at 1195, 1360, and 1655 nm are similar to each other, as there is little asynchronicity between these bands (Figure 7B). The result

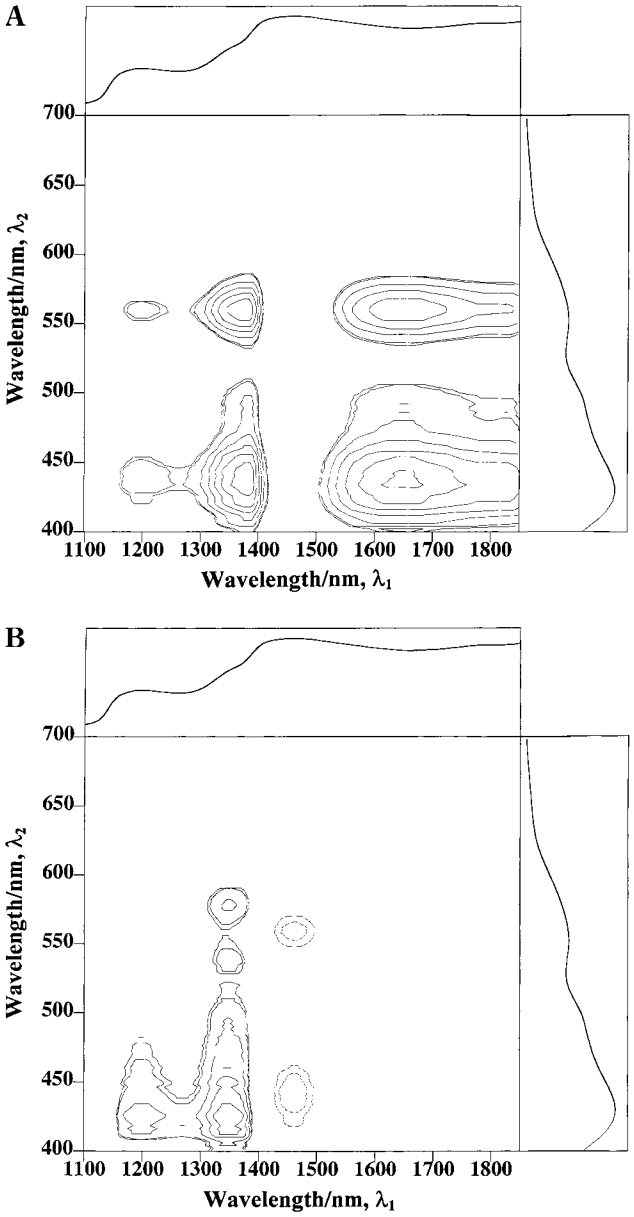

Figure 6. 2D correlation spectra of cooked chicken muscles in the off-diagonal region bounded by 400−700 nm (vertical) and 1100−1850 nm (horizontal): (A) synchronous contour line version; (B) asynchronous contour line version. The corresponding portions of the average spectrum for the data set are plotted at the top and right of each plot.

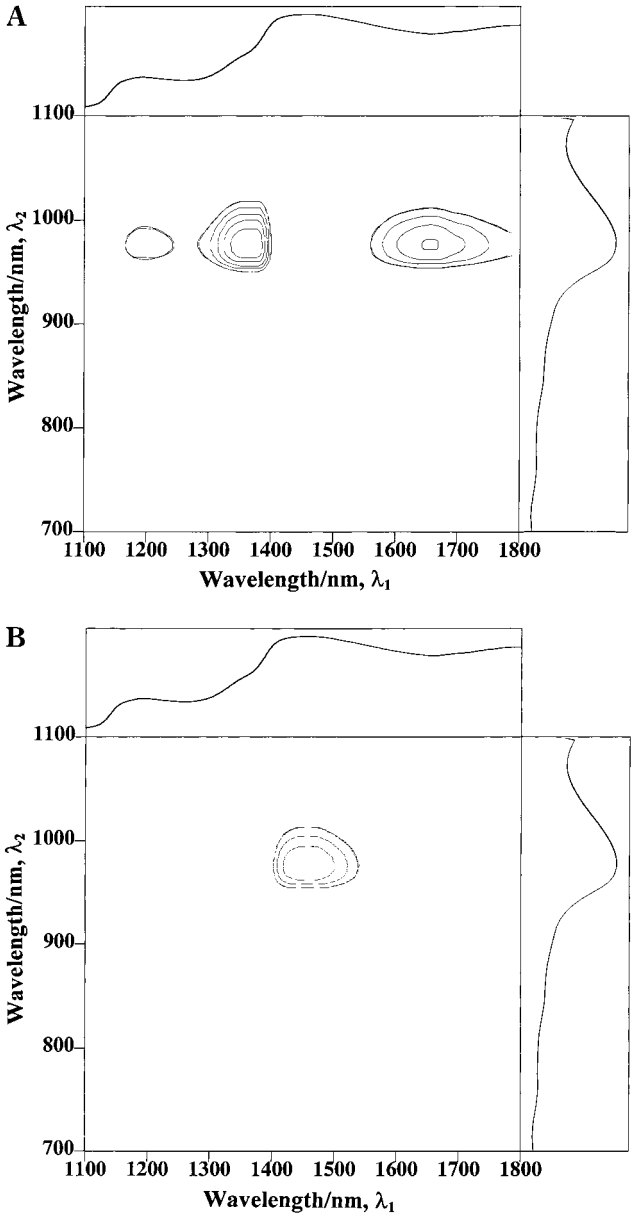

Figure 7. 2D correlation spectra of cooked chicken muscles in the off-diagonal region bounded by 700−1100 nm (vertical) and 1100−1800 nm (horizontal): (A) synchronous contour line version; (B) asynchronous contour line version. The corresponding portions of the average spectrum for the data set are plotted at the top and right of each plot.

indicates that these bands share an identical time-dependent pattern. Hence, the 980, 1195, and 1655 nm bands are probably assigned to the third, second, and first overtones, respectively, of C−H stretching modes of pigment heme groups in both deoxymyoglobin and oxymyoglobin, whereas the 1360 nm band may be due to the combinations of corresponding C−H vibrations.

It can be concluded that the bands at 980, 1195, 1360, and 1655 nm can be assigned to C−H vibration modes of both deoxymyoglobin and oxymyoglobin components. Undoubtedly, other components such as lipid can also contribute to these bands, but, in general, their concentrations are lower than myoglobin and water in breast muscle; therefore, their effects are minimal. In addition, the band due to the second overtone of the O−H stretching mode of water absorbs near 980 nm also (Osborne et al., 1993).

CONCLUSIONS

Visible/NIR spectra are intrinsically very rich in information for studying biological molecular structure and for qualitative and quantitative applications. However, because of their complexity, it is hard to extract useful information from the spectral data alone. The present study has demonstrated for the first time the potential of generalized 2D correlation analysis for the study of thermal processing of meats. A set of visible/NIR spectra of chicken breast under a time (temperature) variation has been investigated by the combination of the synchronous and asynchronous 2D visible/NIR correlation spectra. The existence of a number of bands, especially in the visible region, has been elucidated by the 2D technique. The following conclusions could be drawn from this study.

(1) There are at least seven absorption bands at 415, 425, 445, 475, 520, 560, and 585 nm in the visible region.

The intensities of the bands at 445 and 560 nm, which are assignable to deoxymyoglobin and oxymyoglobin, decrease with cooking. The reduction in their intensities indicates an oxidation and denaturation of deoxymyoglobin and oxymyoglobin into metmyoglobin. The asynchronous 2D correlation spectrum in this visible region implies that one or more bands around 475, 520, and 585 nm may be due to the oxidized/denatured derivatives.

(2) The 2D correlation spectra in the NIR region indicate that the thermally induced decrease in the spectral intensities at 1655, 1195, and 1360 nm, which are attributed to the first and second overtones of C−H stretching modes and combinations of C−H vibrations, respectively, is quite different from that of the 1455 nm band ascribed to the first overtone of the O−H stretching mode of water. From the asynchronous spectrum, it can been concluded that C−H fractions change first before the evaporation of water and dissociation of hydrogen-bonded species, suggesting that heme groups in deoxymyoglobin and oxymyoglobin are easily oxidized and denatured.

(3) Strong correlation peaks appear when the bands between different spectral ranges are correlated. For example, the 445 nm visible band (or 560 nm) is found to be correlated with the SW-NIR band at 980 nm and NIR bands at 1195, 1360, and 1655 nm, implying that these bands share a similar time-dependent pattern and may be related to the same component. Examination of 2D correlation patterns and time dependencies allows assignment of specific absorption bands to chemical species in a mixture spectrum.

LITERATURE CITED

Bonanno, A. S.; Olinger, J. M.; Griffiths, P. R. The origin of band positions and widths in near infrared spectra. In *Near Infrared Spectroscopy, Bridging the Gap between Data and NIR Applications (Proceedings of the 5th International Conferences on Near Infrared Spectroscopy)*; Hildrum, K. L., Isaksson, T., Tandberg, A., Eds.; Ellis Horwood: Chichester, U.K., 1992; pp 19−28.

Burns, D. A., Ciurczak, E. W., Eds. *Handbook of Near-Infrared Analysis*; Dekker: New York, 1992.

Chen, H.; Marks, B. P. Evaluation previous thermal treatment of chicken patties by visible/near-infrared spectroscopy. *J. Food Sci.* **1997**, *62*, 753−756, 780.

Chen, H.; Marks, B. P. Visible/near-infrared spectroscopy for physical characteristics of cooked chicken patties. *J. Food Sci.* **1998**, *63*, 279−282.

Chen, Y. R.; Huffman, R. W.; Park, B.; Nguyen, M. Transportable spectrophotometer system for on-line classification of poultry carcasses. *Appl. Spectrosc.* **1996a**, *50*, 910−916.

Chen, Y. R.; Huffman, R. W.; Park, B. Changes in the visible/near-infrared spectra of chicken carcasses in storage. *J. Food Process Eng.* **1996b**, *19*, 121−134.

Chen, Y. R.; Park, B.; Huffman, R. W.; Nguyen, M. Classification of on-line poultry carcasses with backpropagation neural networks. *J Food Process Eng.* **1998**, *21*, 33−48.

Ebihara, K.; Takahashi, H.; Noda, I. Nanosecond two-dimensional resonance Raman correlation spectroscopy of benzil radical anion. *Appl. Spectrosc.* **1993**, *47*, 1343−1344.

Ellekjaer, M. R.; Isaksson, T.; Solheim, R. Assessment of sensory quality of meat sausages using near-infrared spectroscopy. *J Food Sci.* **1994**, *59*, 456−464.

Francis, F. J.; Clydesdale, F. M. *Food Colorimetry: Theory and Application*; Chapman & Hall: New York, 1975.

Kinsman, D. M., Kotula, A. W., Breidemstein, B. C., Eds. *Muscle Foods*; Chapman & Hall: New York, 1994, and references cited therein.

Lanza, E. Determination of moisture, protein, fat and calorie in raw pork and beef by near-infrared spectroscopy. *J. Food Sci.* **1983**, *48*, 471−474.

Lawrie, R. A. *Meat Science*, 4th ed.; Pergamon Press: Oxford, U.K., 1985.

Liu, Y.; Ozaki, Y.; Noda, I. Two-dimensional Fourier-transform correlation spectroscopy study of dissociation of hydrogen-bonded N-methylacetamide in the pure liquid state. *J. Phys. Chem.* **1996**, *100*, 7326−7332.

Liu, Y.; Chen, Y. R.; Ozaki, Y. Characterization of visible spectral intensity variations of wholesome and unwholesome chicken meats with two-dimensional correlation spectroscopy. *Appl. Spectrosc.* **2000**, in press.

Mitsumoto, M.; Maeda, S.; Mitsuhashi, T.; Ozawa, S. Near-infrared spectroscopy determination of physical and chemical characteristics in beef cuts. *J. Food Sci.* **1991**, *56*, 1493−1496.

Nabet, A.; Pezolet, M. Two-dimensional FT-IR spectroscopy: A powerful method to study the secondary structure of proteins using H-D exchange. *Appl. Spectrosc.* **1997**, *51*, 466−469.

Nakano, T.; Shimada, S.; Saitoh, R.; Noda, I. Transit 2D IR correlation spectroscopy of the photopolymerization of acrylic and epoxy monomers. *Appl. Spectrosc.* **1993**, *47*, 1337−1342.

Noda, I. Two-dimensional infrared spectroscopy of synthetic and biopolymers. *Bull. Am. Phys. Soc.* **1986**, *31*, 520.

Noda, I. Two-dimensional vibrational spectroscopy. *J. Am. Chem. Soc.* **1989**, *111*, 8116−8117.

Noda, I. Two-dimensional infrared (2D IR) spectroscopy: Theory and applications. *Appl. Spectrosc.* **1990**, *44*, 550−561.

Noda, I. Generalized two-dimensional correlation method applied to infrared, Raman, and other types of spectroscopy. *Appl. Spectrosc.* **1993**, *47*, 1329−1336.

Noda, I. *Abstract of Papers in 2nd International Symposium on Advanced Infrared Spectroscopy*; Durham, NC, 1996a.

Noda, I. Thesis for the Degree of Doctor of Science, The University of Tokyo, Tokyo, 1996b.

Noda, I.; Liu, Y.; Ozaki Y.; Czarnecki, M. A. Two-dimensional Fourier transform near-infrared correlation spectroscopy studies of temperature-dependent spectral variations of oleyl alcohol. *J. Phys. Chem.* **1995**, *99*, 3068−3073.

Noda, I.; Liu, Y.; Ozaki, Y. Two-dimensional correlation spectroscopy study of temperature-dependent spectral variations of N-methylacetamide in the pure liquid state. 1. Two-dimensional infrared analysis. *J. Phys. Chem.* **1996a**, *100*, 8665−8673.

Noda, I.; Liu, Y.; Ozaki, Y. Two-dimensional correlation spectroscopy study of temperature-dependent spectral variations of N-methylacetamide in the pure liquid state. 2. Two-dimensional Raman and infrared-Raman heterospectral analysis. *J Phys. Chem.* **1996b**, *100*, 8674−8680.

Osborne, B. G.; Fearn, T.; Hindle, P. H. *Practical Near-Infrared Spectroscopy with Application in Food and Beverage Analysis*, 2nd ed.; Wiley: New York, 1993.

Ozaki, Y.; Liu, Y.; Noda, I. Two-dimensional near-infrared correlation spectroscopy study of premelting behavior of Nylon 12. *Macromolecules* **1997**, *30*, 2391−2399.

Park, B.; Chen, Y. R.; Hruschka, W. R.; Shackelford, S. D.; Koohmaraie, M. Near-infrared reflectance analysis for predicting beef longissimus tenderness. *J. Anim. Sci.* **1998**, *76*, 2115−2120.

Price, J.; Schweigert, B. *The Science of Meat and Meat Products*, 3rd ed.; Food and Nutrition Press: Westport, CT, 1987.

Sefara, N. L.; Magtoto, N. P.; Richardson, H. H. Structural characterization of β-lactoglobulin in solution using two-dimensional FT mid-Infrared and FT near-infrared correlation spectroscopy. *Appl. Spectrosc.* **1997**, *51*, 536−540.

Silverstein, P. M.; Bassler, G. C.; Morrill, T. C. *Spectrometric Identification of Organic Compounds*, 5th ed.; Wiley: New York, 1991.

Swatland, H. J. Fiber optic spectrophotometry of color changes in cooked chicken muscles. *Poult. Sci.* **1983**, *62*, 957−959.

Swatland, H. J. A review of meat spectrophotometry (300 to 800 nm). *Can. Inst. Food Sci. Technol. J.* **1989**, *22*, 390−402.

Wang, Y.; Murayama, K.; Myojo, Y.; Tsenkova, R.; Hayashi, N.; Ozaki, Y. Two-dimensional Fourier transform near-infrared spectroscopy study of heat denaturation of ovalbumin in aqueous solutions. *J. Phys. Chem. B* **1998**, *102*, 6655−6662.

Williams, P., Norris, K., Eds. *Near-infrared Technology in the Agricultural and Food Industrious*; American Association of Cereal Chemists: St. Paul, MN, 1990.

Received for review June 18, 1999. Revised manuscript received November 16, 1999. Accepted December 2, 1999. Mention of a product or specific equipment does not constitute a guarantee or warranty by the U.S. Department of Agriculture and does not imply its approval to the exclusion of other products that may also be suitable.

JF990662B